

Supporting Information

Design of Anti-PD-L1 Mediated MOF Nanodrug Delivery System Using Terpyridine-Metal Coordination for Tumor Theranostics

Xu Han, Jia Chen, Zhihao Cheng, and Shengwang Zhou *

School of Pharmacy, Jiangsu University, Zhenjiang 212013, P. R. China.

Corresponding Author

*Email: shengwangzhou@ujs.edu.cn

Experimental Section

Materials

1,3,5-Benzenetricarboxylic acid, cystamine dihydrochloride, 3-(4,5-dimethyl-2-thiazolyl)-2,5-diphenyl tetrazolium bromide, and N-hydroxy succinimide were purchased from Aladdin Reagents (Shanghai, China). Polyvinyl pyrrolidone, xylene orange, copper nitrate trihydrate, and gadolinium (III) chloride hexahydrate were purchased from Shanghai Macklin Biochemical Technology Co., Ltd. Purified anti-PD-L1 antibody was obtained from Elabscience (USA). L-glutathione (reduced), bis(cyclohexanone) oxalyldihydrazone, 1-(3-dimethylaminopropyl)-3-ethylcarbodiimide hydrochloride, and 2,2':6',2''-terpyridine-4'-carboxylic acid were purchased from Shanghai Titan Scientific Co., Ltd.

Instruments and Characterizations

The morphology and microstructure were investigated using a field emission scanning electron microscope (FESEM, 7001F, JEOL). Transmission electron microscopy images were obtained with a Hitachi H-7500 microscope. Nitrogen adsorption/desorption isotherms were acquired on the Quantachrome NOVA 3000e analyzer. UV-visible absorption spectra were measured by a UV-visible spectrophotometer (Metash, UV-8000). FTIR analysis was performed on a Thermo Nicolet Avatar-370 spectrometer. CLSM images were captured with a Leica TCS SP5 confocal laser scanning microscope. X-ray powder diffraction (XRD) measurements were conducted using a Bruker D8 ADVANCE X-ray diffractometer with Cu K α radiation. In vivo imaging of mice was carried out using the Bruker In-Vivo Xtreme II system, and MR images were captured with a 7.0 T Bruker BioSpec imaging system. Elemental analysis was conducted using X-ray photoelectron spectroscopy (XPS, ESCALAB 250xi).

Synthesis of Cu-MOF and Tpy-SS-MOF

Cu(NO₃)₂·3H₂O (2.0 g, 8.3 mmol) and 1.0 g PVP (MW 58000) were dissolved in 250 ml methanol. The solution was sonicated, after which 1,3,5-benzenetricarboxylic acid (1.1 g,

5.2 mmol) was added and the mixture was allowed to stand at room temperature for 24 hours. Subsequently, the sediment was washed with ethanol (3×30ml) and dried in a vacuum oven at 60°C for 24 hours to obtain Cu-MOF.

Cu-MOF (0.1 g) was dispersed in 10 mL of aqueous solution, and EDC (23.25 mg, 0.15 mmol) and NHS (17.26 mg, 0.15 mmol) were added. The mixture was stirred at room temperature for 6 hours, after which cystamine dihydrochloride (33.78 mg, 0.15 mmol) was introduced and stirred for an additional 6 hours. The product was washed three times with deionized water and centrifuged to isolate the functionalized Cu-MOF, which had disulfide bonds on its surface. Subsequently, 20 mg of the functionalized MOF was dispersed in 10 mL of aqueous solution, and 10 mL of DMSO solution containing 2,2':6',2''-terpyridine-4-carboxylic acid (33.75 mg, 0.15 mmol) was added. The suspension was stirred for 12 hours, after which the solids were collected, washed three times with deionized water, centrifuged, and dried to obtain Tpy-SS-MOF.

Construction of CPT-loaded anti-PD-L1@Tpy-SS-MOF nanodrug delivery system

Anti-PD-L1 was pretreated using the following procedure: 2,2':6',2''-Terpyridine-4'-carboxylic acid (3.375 mg, 0.015 mmol) was dissolved in 0.5 mL of Tris-HCl buffer, followed by the addition of EDC and NHS. This mixture was stirred at room temperature for 6 hours. The reaction temperature was then reduced to 0°C, and purified anti-PD-L1 (0.5 mL, 0.5 mg/mL) was introduced and stirred for an additional 6 hours, allowing for the covalent coupling of 2,2':6',2''-Terpyridine-4'-carboxylic acid with anti-PD-L1.

In a separate step, Tpy-SS-MOF (10 mg) was added to a CPT loading solution (10 mL, 0.2 mM) and stirred at room temperature for 12 hours to facilitate the complete adsorption and encapsulation of CPT within the Tpy-SS-MOF. The resulting CPT-loaded Tpy-SS-MOF was then washed with Tris-HCl buffer for purification. Subsequently, the pretreated anti-PD-L1 was added (1 mL, 0.25 mg/mL), followed by GdCl₃ solution (1mL, 0.03M). After stirring for 12 hours, the antibody was bonded to the MOF surface through Tpy-Gd³⁺-Tpy coordination chemistry. The precipitate was then centrifuged and thoroughly washed with

Tris-HCl to obtain the CPT-loaded anti-PD-L1@Tpy-SS-MOF.

The loading capacities of CPT within anti-PD-L1@Tpy-SS-MOF

Tpy-SS-MOF (10 mg) was dispersed in a 10 ml solution of CPT (0.2 mM). Anti-PD-L1 with Tpy ligands was then introduced to enable nanogate formation. Following a 12-hour incubation, the solution was centrifuged to separate the solid precipitate from the supernatant, which was subsequently collected. The precipitate was rinsed thoroughly with Tris-HCl buffer, and the rinse solution was combined with the supernatant. The fluorescence intensity of the combined solution (60 ml) was measured using a fluorescence spectrometer, with final concentration determined via comparison to a CPT standard curve (Fig. S8). CPT loading capacity in anti-PD-L1@Tpy-SS-MOF was quantified by calculating the difference between initial and remaining CPT amounts.

The stimuli responsive controlled release of CPT

The kinetics of CPT release were monitored through fluorescence measurements ($\lambda_{\text{ex}} = 365$ nm, $\lambda_{\text{em}} = 440$ nm). For the experiments, 3.5 mg of anti-PD-L1@Tpy-SS-MOF was dissolved in 4 ml of Tris-HCl buffer (pH 7.4), and release profiles were obtained under various triggering conditions. First, drug release was examined at acidic pH levels (pH 3.0 and 5.0) by adding 1 M hydrochloric acid. Next, the release kinetics were measured in the presence of 5 mM glutathione (GSH). Finally, the combined effect of acidic pH (3.0) and GSH (5 mM) was evaluated by adding GSH to the solution adjusted to pH 3.0.

Assessment of Gd³⁺ concentration in anti-PD-L1@Tpy-SS-MOF

To quantify the Gd³⁺ concentration in the anti-PD-L1@Tpy-SS-MOF nanodrug delivery system, we conducted a spectrophotometric quantification experiment to analyze the Gd³⁺ content following coordination interactions. 10 mg of Tpy-SS-MOF was suspended in a 1.5 mM GdCl₃ solution (20 mL). Subsequently, anti-PD-L1 conjugated with Tpy ligands was introduced, and the mixture was stirred for 12 hours. After centrifugation, the residual loading buffer was collected for spectrophotometric analysis. Spectrophotometric quantification of Gd³⁺ is based on the differences in the UV-Vis spectra between free

xylene orange (XO) dye and its complexed form (Fig S5). The calibration curve depicting the UV-Vis absorption of xylene orange at 570 nm with varying Gd^{3+} concentrations is shown in Fig. S5. The residual Gd^{3+} concentration in the loading solution after chelation was determined to be 0.02615 mmol (Fig. S5). By calculating the concentration change of Gd^{3+} in the solution before and after chelation, the Gd cation concentration incorporated into the anti-PD-L1@Tpy-SS-MOF nanodrug delivery system was determined to be 0.385 mmol/g.

Assessment of Gd^{3+} -Tpy coordination interactions within the nanodrug delivery system at pH 3.0

To investigate the coordination bonds between Gd^{3+} and Tpy at pH levels below 3.0, we conducted the experiment as follows. 10 mg of anti-PD-L1@Tpy-SS-MOF was dispersed in water and stirred for 6 hours at pH 3.0. Subsequently, the solid was removed, and the supernatant was collected for UV-Vis analysis. The UV-Vis spectra of anti-PD-L1@Tpy-SS-MOF at pH 3.0 displayed the characteristics of the Gd^{3+} -XO complex, confirming the presence of free Gd^{3+} in the solution at this pH level. We also prepared a $GdCl_3$ solution (20 mL) corresponding to the Gd content in 10 mg of Tpy-SS-MOF (0.385 mmol/g). Furthermore, the absorption intensity of the Gd^{3+} -XO complex at pH 3.0 was slightly lower than that corresponding to the amount of loaded Gd^{3+} (Fig. S15), indicating that most of the Tpy- Gd^{3+} coordination bonds were disrupted at this pH.

Evaluation of Cu^{2+} ion release in the nanodrug delivery system across pH 3 to 7

We utilized ultraviolet-visible (UV-Vis) spectroscopy to determine Cu^{2+} concentrations, employing the absorbance properties resulting from the interaction between bis(cyclohexanone) oxalyldihydrazone (BCO) and Cu^{2+} . 3 mg of Tpy-SS-MOF was dispersed in 3 mL of water, and the pH was subsequently adjusted to 7.0, 5.0, and 3.0. After a 24-hour incubation, the solid was removed, and the supernatant was collected for UV-Vis analysis. The results of the analysis indicated the final Cu^{2+} concentrations in the nanodrug delivery system (Fig. S13 and S14), which were found to be 1.1, 7.3, and 12.7

$\mu\text{g/mL}$ at pH levels of 7.0, 5.0, and 3.0 for anti-PD-L1@Tpy-SS-MOF (1 mg/mL), respectively. This observation reveals that Cu^{2+} release from the nanodrug delivery system is negligible in a physiological environment.

Cell culture and in vitro cell cytotoxicity

Cytotoxicity assays and CLSM imaging were performed using AGS cells (PD-L1 positive) and HepG2 cells (PD-L1 negative). The cells were cultured in DMEM medium containing 10% fetal bovine serum, along with dual antibiotics: streptomycin (100 $\mu\text{g/ml}$) and penicillin (100 U/ml). Cell cultures were maintained in an incubator at 37°C with 5% CO_2 . To prepare for the assays, the cells were seeded in 96-well plates at a density of 1×10^6 cells per well and incubated for 24 hours. Subsequently, nanoparticles were introduced at final concentrations of 10, 20, 40, 100, 200, and 300 $\mu\text{g/ml}$, and the cells were incubated for an additional 24 hours. Cell viability was determined using the MTT assay, with absorbance values measured by an ELISA microplate reader.

CLSM analysis of cellular drug uptake

AGS and HepG2 cells were plated in confocal culture dishes, and 100 $\mu\text{g/ml}$ of CPT-loaded anti-PD-L1@Tpy-SS-MOF was added to each well. The drug release behavior was monitored using CLSM after incubation periods of 3, 6, 12, and 24 hours, capturing fluorescence images under the CPT optical window ($\lambda_{\text{ex}} = 365 \text{ nm}$, blue).

In vitro MRI characterization of the anti-PD-L1@Tpy-SS-MOF nanodrug delivery system

The anti-PD-L1@Tpy-SS-MOF contains Gd(III) chelates, making it suitable for magnetic resonance imaging. The magnetic resonance properties of the anti-PD-L1@Tpy-SS-MOF nanoparticles were assessed at the solution level by measuring their longitudinal (T_1) and transverse (T_2) relaxation times across various concentrations. Solutions of MOF nanoparticles were prepared at concentrations of 25, 50, 100, 200, and 300 $\mu\text{g/ml}$ using ultrapure water as the solvent. The inverse relaxation times ($1/T_1$ and $1/T_2$) were plotted against the nanoparticle concentrations, and linear fitting was applied to determine the

relaxivity values (r_1 and r_2). The repetition time (TR) was set to 600.0 ms, and the echo time (TE) was set to 18.0 ms for the imaging experiments.

In vivo antitumor efficacy of combination therapies in tumor-bearing mice

When the tumor volume of xenograft mice (HepG2 or AGS-bearing) reached approximately 100 mm³, the mice were randomly assigned to three groups (n = 3 per group) for treatment via tail vein injection. The treatment groups received twice-daily injections of PBS, anti-PD-L1@Tpy-SS-MOF without CPT, and CPT-loaded anti-PD-L1@Tpy-SS-MOF at a dosage of 5 mg·kg⁻¹. Tumor growth and body weight were monitored every two days, and tumor volumes were calculated. At the end of the study, tumors were dissected for gravimetric analysis and H&E staining.

Live Subject Statement

BALB/c mice (~6 weeks) were purchased from Cavens Company (Changzhou, China). All related animal experiments were performed in compliance with the relevant laws of China and the institutional guidelines of Jiangsu University. The experiments involving mice were approved by The Institutional Animal Care and Use Committee of Jiangsu University (UJS IACUC), with ethics approval number UJS-IACUC-2023112401.

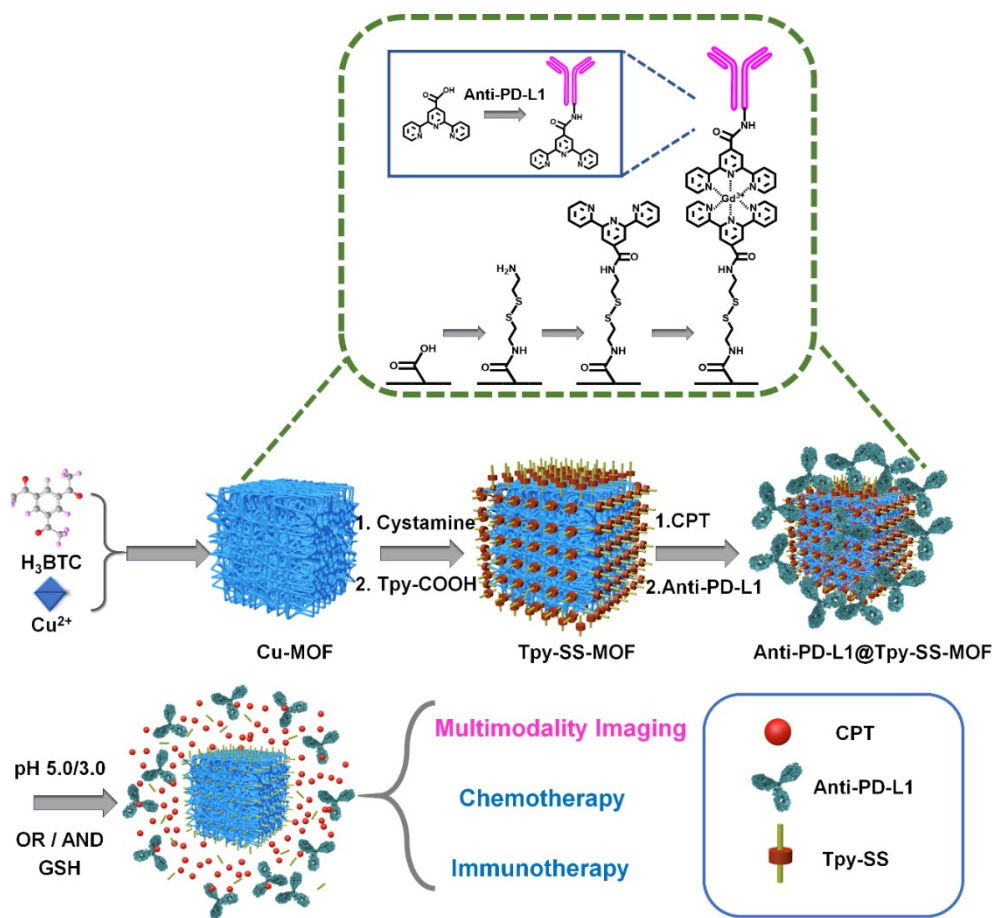


Fig. S1. A schematic illustrates the development of an anti-PD-L1@Tpy-SS-MOF nanodrug delivery system for integrated tumor diagnosis and combination therapy. The Cu-MOF was surface-modified using solid-phase chemical modification techniques, and antibody nanogates were constructed via Tpy-Gd³⁺-Tpy conjugation on the MOF surface through coordination chemistry. The anti-PD-L1 mediated nanodrug delivery system targets tumors by recognizing overexpressed antigens, utilizing mechanisms such as cell binding and T-cell activation for tumor therapy. It facilitates accurate tumor diagnosis through fluorescence (FL) and magnetic resonance (MR) imaging. Upon GSH reduction or acidic conditions, conjugation bonds are cleaved, releasing CPT and antibodies.

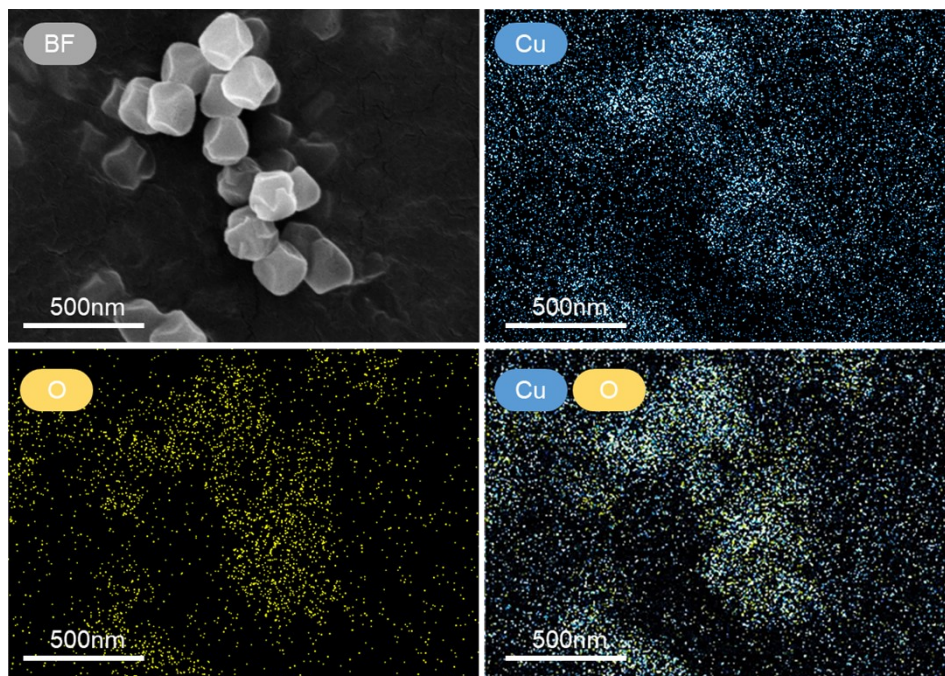


Fig. S2. Elemental mapping of Cu-MOF using energy-dispersive X-ray spectroscopy (EDS). The EDS-colored element maps show Cu in blue and O in yellow.

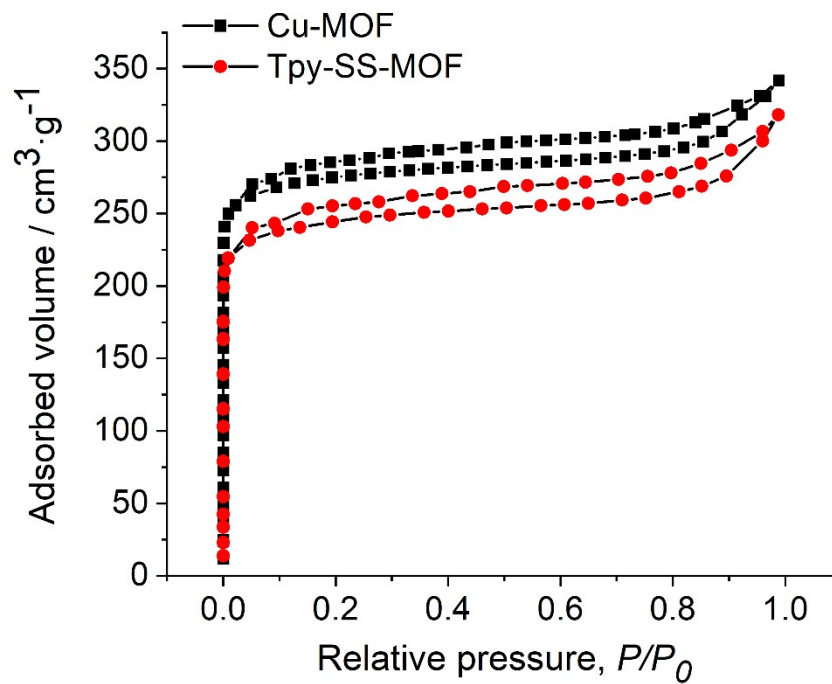


Fig. S3. Nitrogen adsorption-desorption isotherms of Cu-MOF and Tpy-SS-MOF.

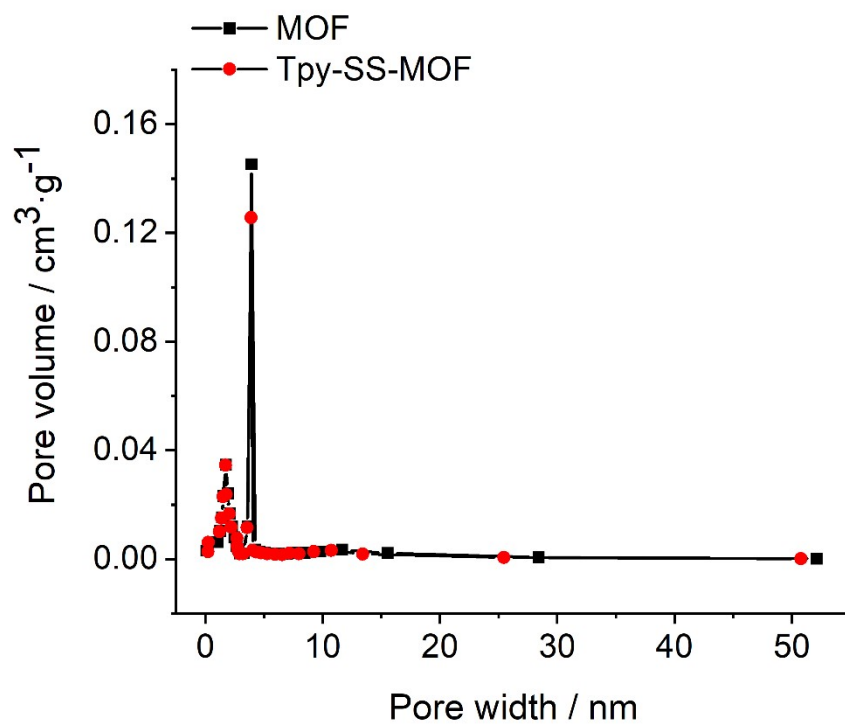


Fig. S4. Pore size distributions of Cu-MOF and Tpy-SS-MOF.

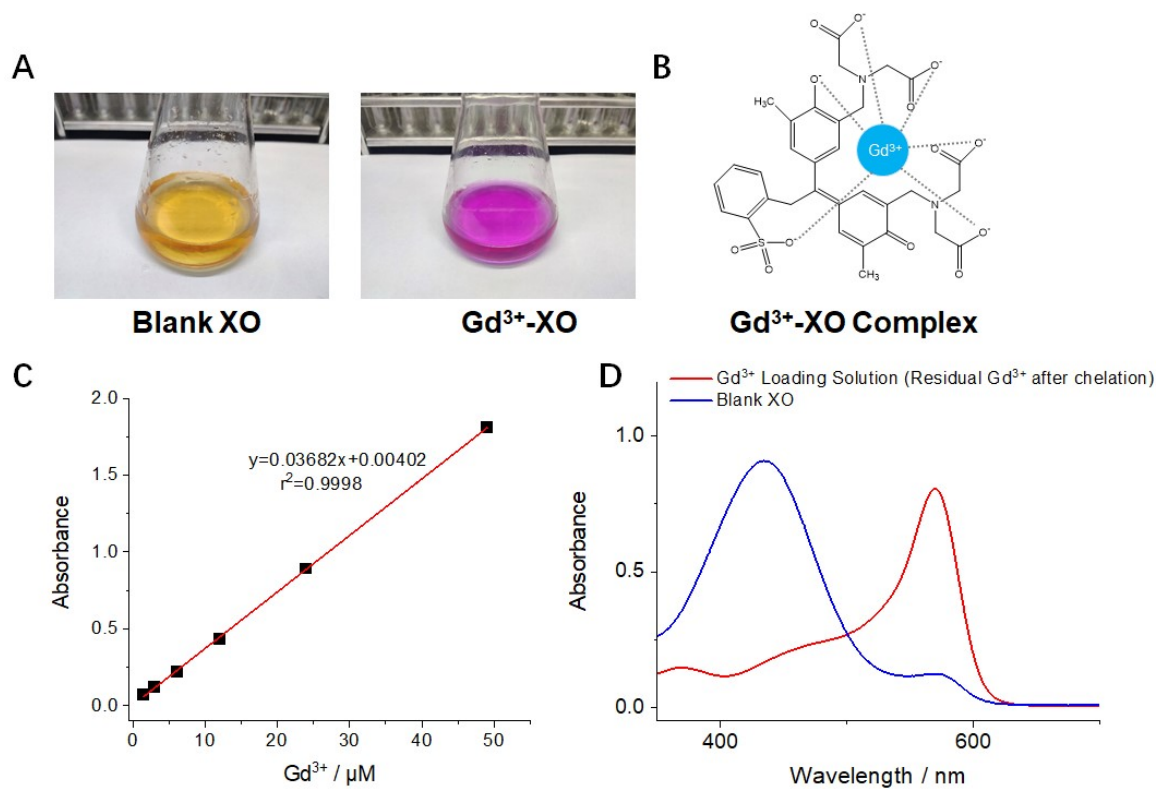


Fig. S5. (A) The representative color photographs of blank xylenol orange (XO) and the

Gd³⁺-XO complex. (B) The molecular formula of the Gd³⁺-XO complex. (C) Calibration curve depicting the UV-Vis absorption of xylenol orange at 570 nm with varying Gd³⁺ concentrations. (D) UV-Vis spectrum of blank XO (blue); UV-Vis spectrum of the Gd³⁺ loading solution after chelation (red, 1:60 dilution), illustrating the residual Gd³⁺ detected through complexation with XO.

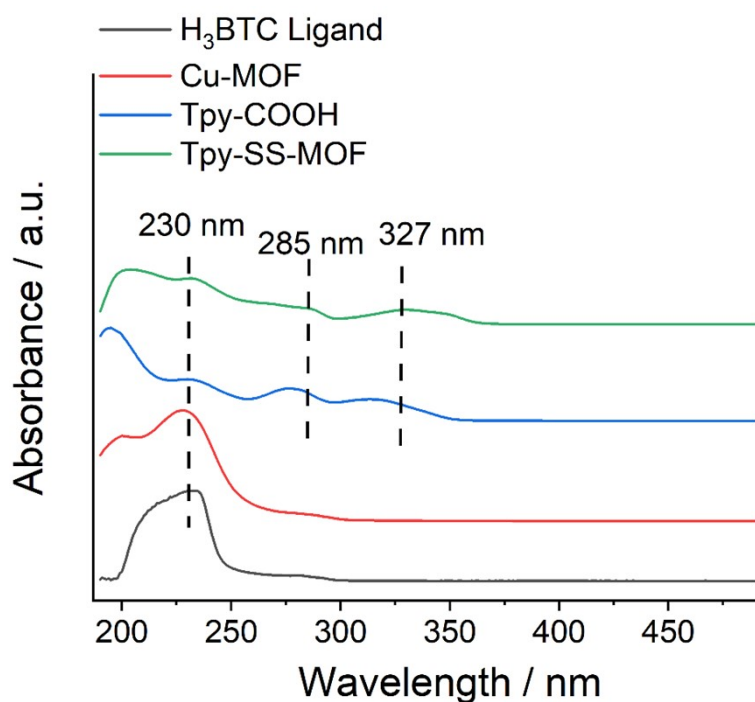


Fig. S6. UV-vis absorption spectra of the H₃BTC ligand, synthesized Cu-MOF, Tpy-COOH, and Tpy-SS-MOF.

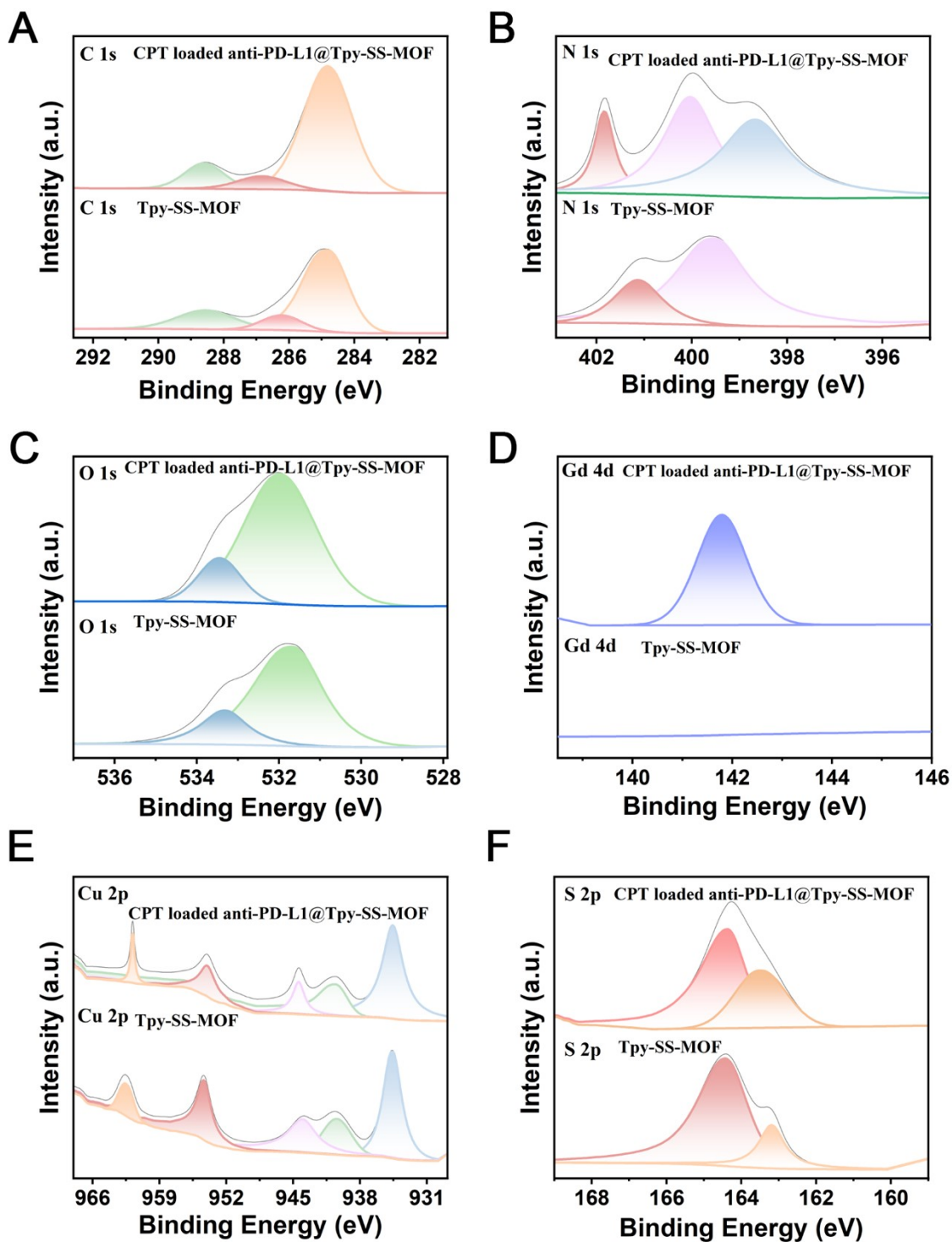


Fig. S7. XPS analysis of Tpy-SS-MOF and CPT loaded anti-PD-L1@Tpy-SS-MOF. (A) C 1s, (B) N 1s, (C) O 1s, (D) Gd 4d, (E) Cu 2p, and (F) S 2p.

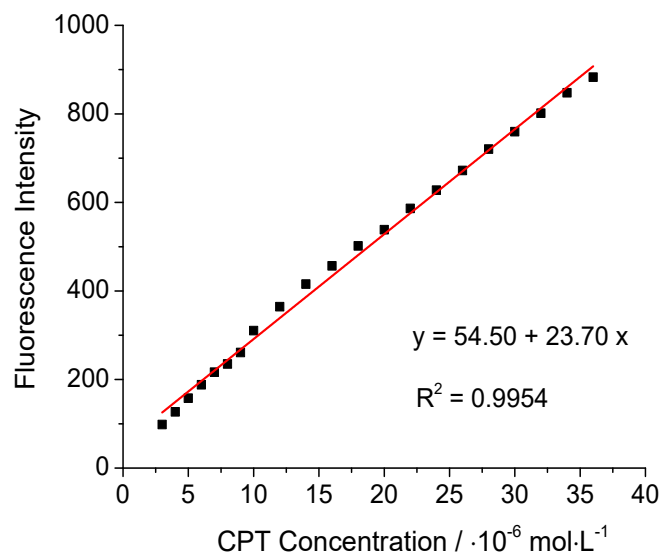


Fig. S8. The standard curve of CPT fluorescence intensity was generated by plotting the fluorescence intensity versus the concentration of CPT. The fluorescence intensity of CPT was measured using a fluorescence spectrometer.

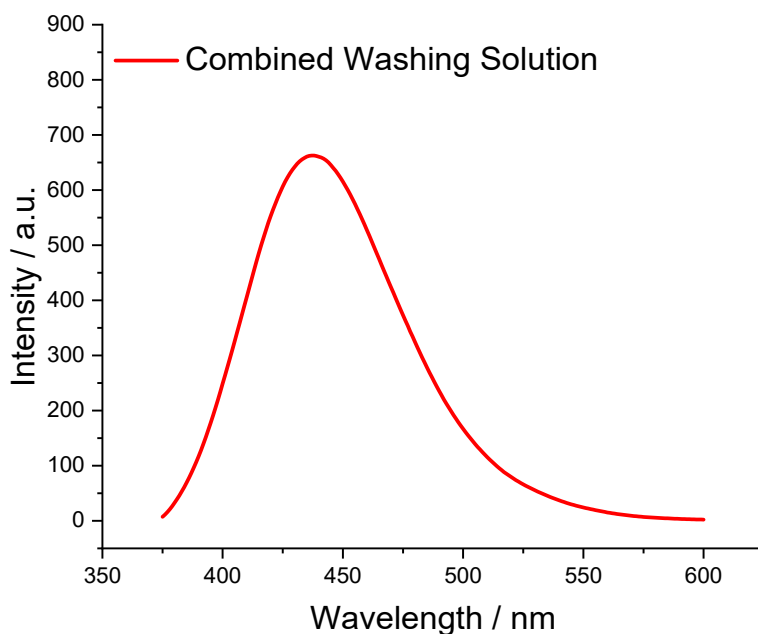


Fig. S9. Fluorescence spectrum of the combined washing solution containing CPT in 60 mL Tris-HCl solution ($\lambda_{\text{ex}} = 365 \text{ nm}$, $\lambda_{\text{em}} = 440 \text{ nm}$)

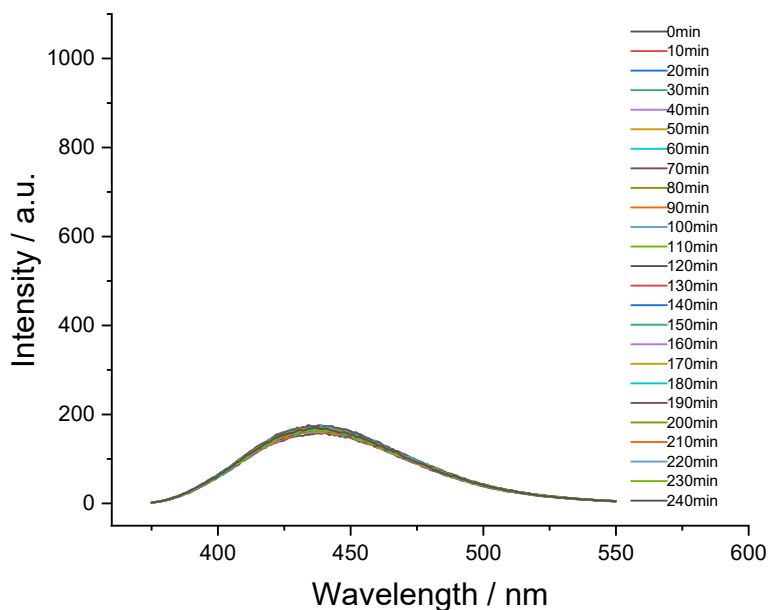


Fig. S10. Fluorescence spectra of CPT released from non-triggered anti-PD-L1@Tpy-SS-MOF in a Tris-HCl solution ($\lambda_{\text{ex}} = 365 \text{ nm}$).

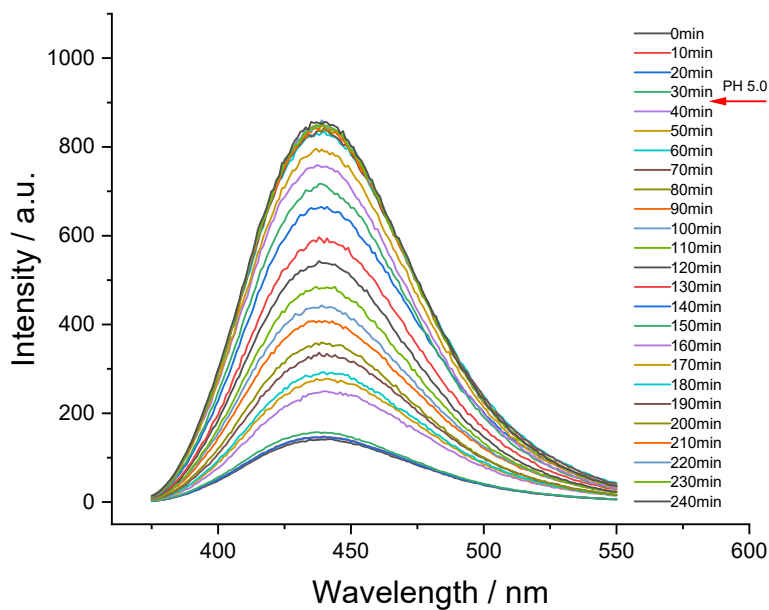


Fig. S11. Fluorescence spectra of CPT released from CPT-loaded anti-PD-L1@Tpy-SS-MOF in a Tris-HCl solution triggered by a pH change from 7.4 to 5.0 after 30 minutes ($\lambda_{\text{ex}} = 365 \text{ nm}$).

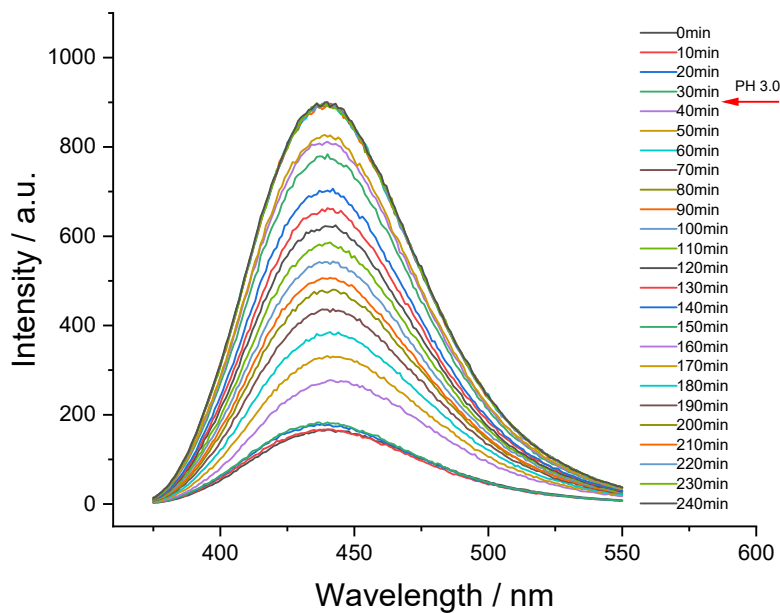


Fig. S12. Fluorescence spectra of CPT released from CPT-loaded anti-PD-L1@Tpy-SS-MOF in a Tris-HCl solution triggered by a pH change from 7.4 to 3.0 after 30 minutes ($\lambda_{\text{ex}} = 365 \text{ nm}$).

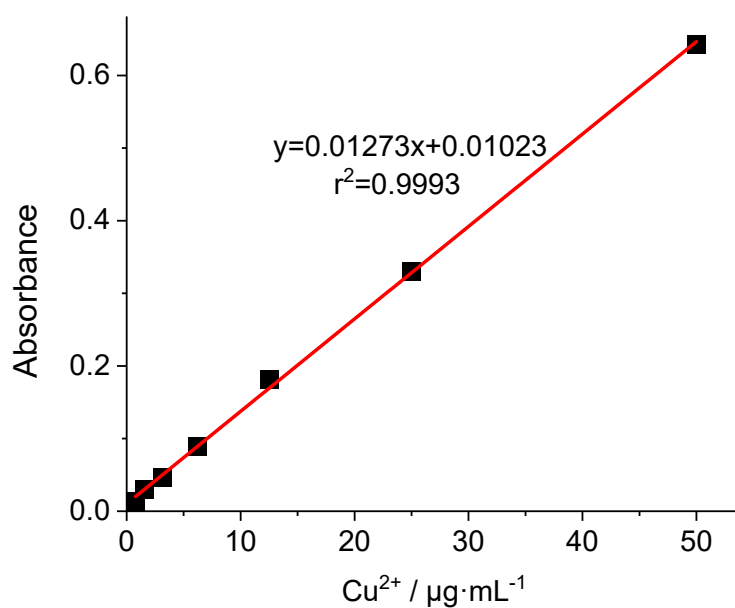


Fig. S13. The standard calibration curve of the complex generated by Cu^{2+} ions and bis(cyclohexanone) oxalyldihydrazone illustrates the correlation between the concentration of copper ions and the resulting complex. Absorbance was measured at an excitation wavelength of 600 nm using a spectrophotometer.

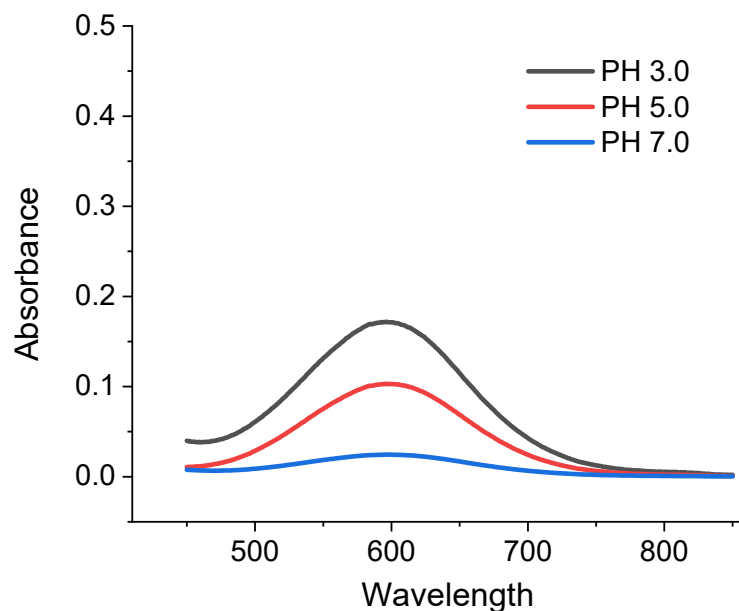


Fig. S14. UV-Vis spectrum of Cu^{2+} with the indicator bis(cyclohexanone) oxalyldihydrazone from the nanodrug delivery system after a 24-hour incubation at pH levels of 7.4, 5.0, and 3.0.

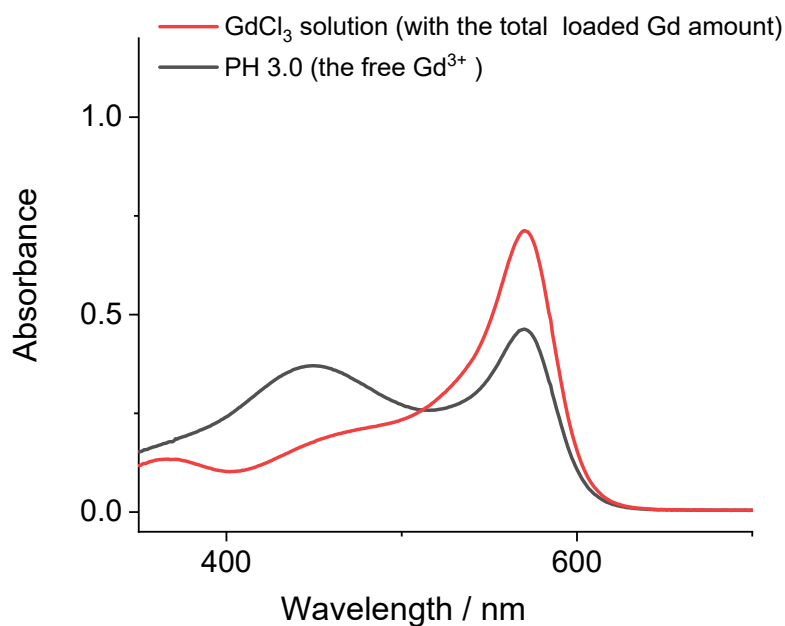


Fig. S15. UV-Vis spectrum of the GdCl_3 solution with the total loaded Gd amount (red, 1:10 dilution); UV-Vis spectrum of the supernatant solution from anti-PD-L1@Tpy-SS-MOF after 6 hours of incubation at pH 3.0 (black, 1:10 dilution), illustrating the detection of free Gd^{3+} ions through complexation with XO.

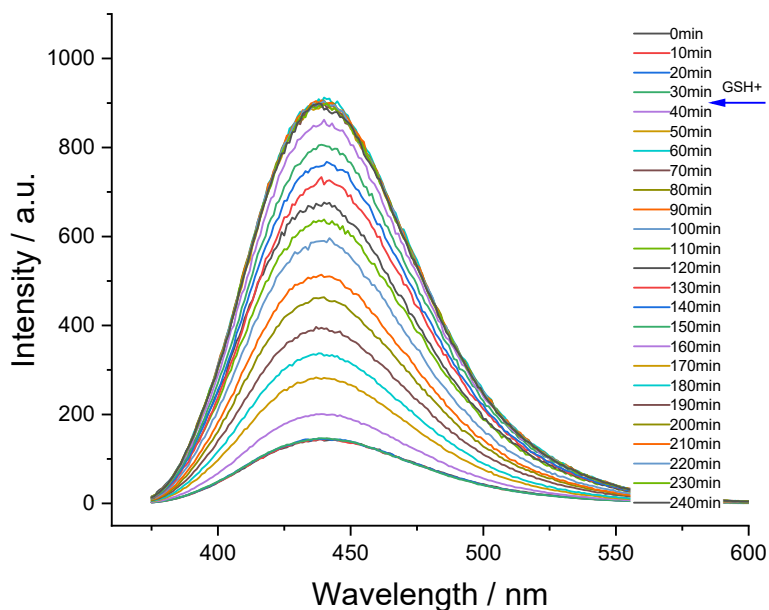


Fig. S16. Fluorescence spectra of CPT released from CPT-loaded anti-PD-L1@Tpy-SS-MOF in Tris-HCl solution with GSH (5 mM) added at 30 minutes ($\lambda_{\text{ex}} = 365 \text{ nm}$).

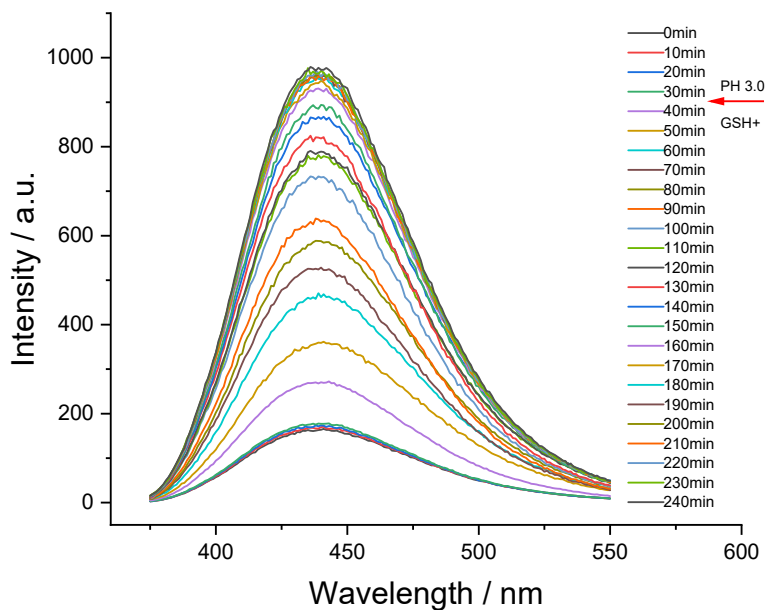


Fig. S17. Fluorescence spectra of CPT released from CPT-loaded anti-PD-L1@Tpy-SS-MOF in Tris-HCl solution in the presence of both triggers of pH 3.0 and GSH (5 mM), which were introduced at 30 minutes ($\lambda_{\text{ex}} = 365 \text{ nm}$).

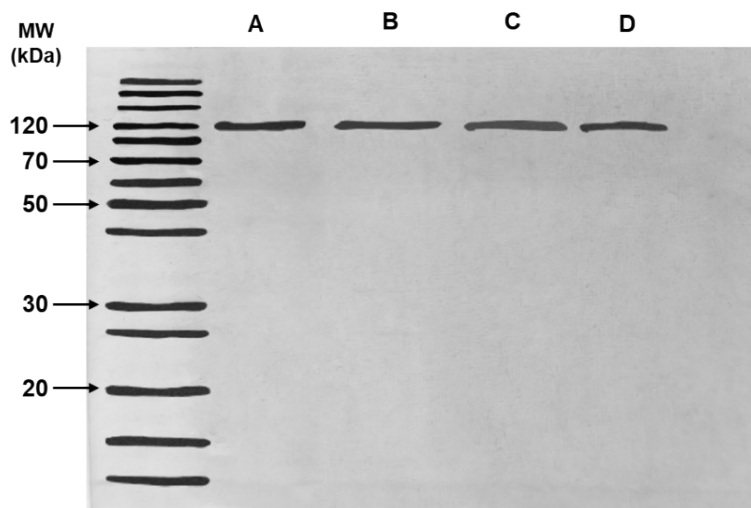


Fig. S18. SDS-PAGE analysis of (A) pure anti-PD-L1, antibody release in the supernatant triggered at (B) pH 5.0, (C) pH 3.0, and (D) in the presence of 5 mM GSH.

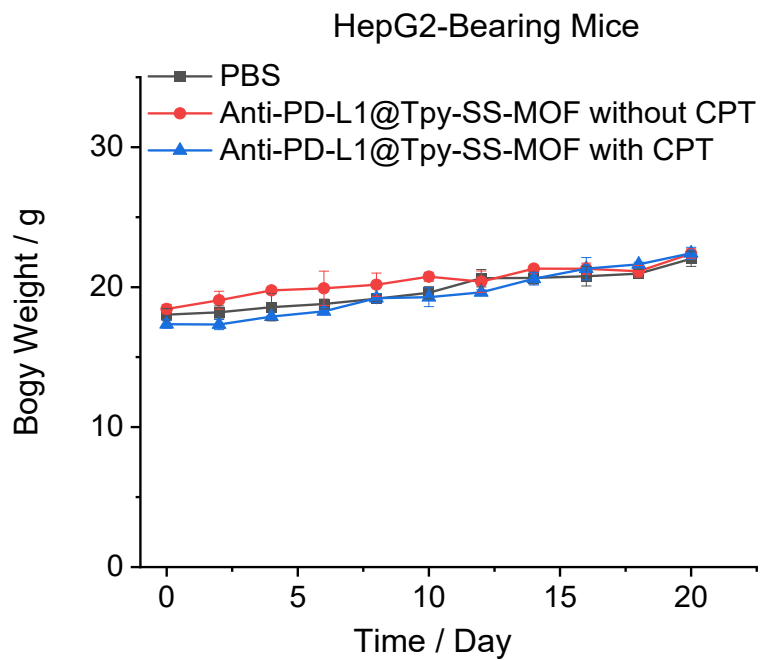


Fig. S19. Body weight variations in HepG2-bearing mice during a 20-day treatment period involving the administration of CPT-loaded anti-PD-L1@Tpy-SS-MOF nanodrugs.

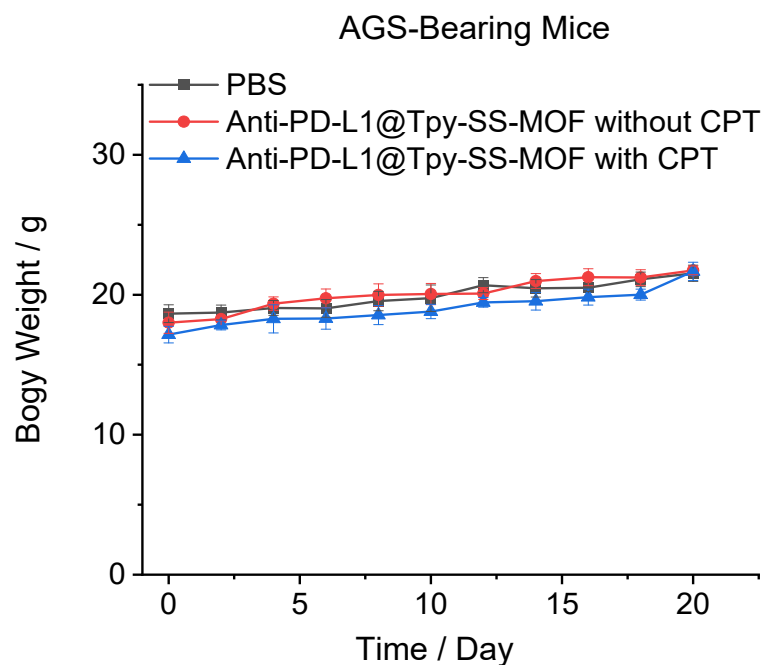


Fig. S20. Body weight variations in AGS-bearing mice during a 20-day treatment period involving the administration of CPT-loaded anti-PD-L1@Tpy-SS-MOF nanodrugs.

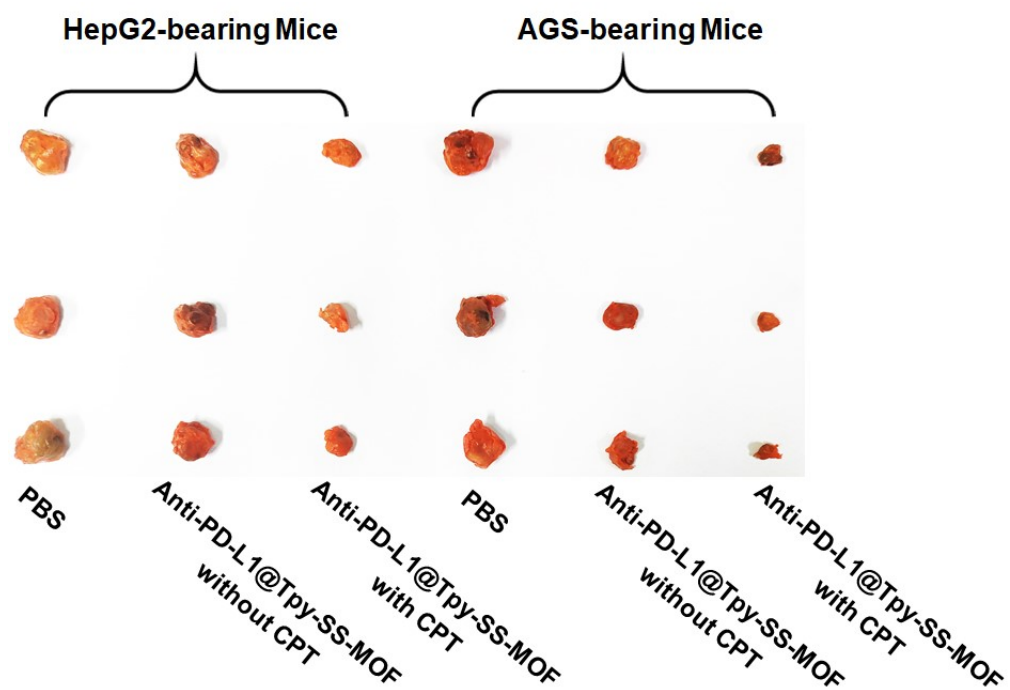


Fig. S21. Representative images showing tumors obtained from tumor-bearing mice at the end of the treatment phase.

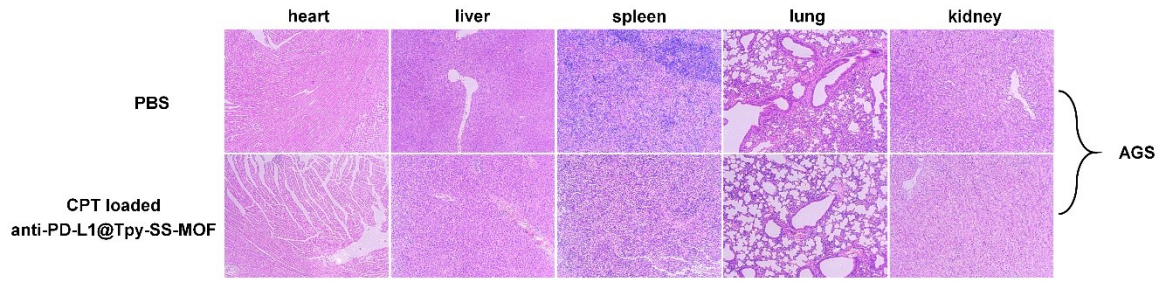


Fig. S22. H&E staining images of the primary organs (heart, liver, spleen, lung, and kidney) from AGS-bearing mice at the end of the treatment phase involving CPT-loaded anti-PD-L1@Tpy-SS-MOF nanodrugs.